Astragaloside IV protects against autoimmune myasthenia gravis in rats via regulation of mitophagy and apoptosis

JINGJING ZHANG[1,2], JIAYAN HUANG[1,2], JINLIAN LAN[1,2], QING LI[1,2], LINGLING KE[1,2], QILONG JIANG[3], YANWU LI[1,2], HAN ZHANG[4], HUIYA ZHONG[1,2], PEIDAN YANG[1,2], TONGKAI CHEN[1] and YAFANG SONG[1,2]

[1]Science and Technology Innovation Center, Guangzhou University of Chinese Medicine, Guangzhou, Guangdong 510405, P.R. China; [2]Institute of Pi-Wei, Guangzhou University of Chinese Medicine, Guangzhou, Guangdong 510405, P.R. China; [3]Department of Gastrosplenic Diseases, The First Affiliated Hospital of Guangzhou University of Chinese Medicine, Guangzhou, Guangdong 510405, P.R. China; [4]School of Chinese Materia Medica, Guangdong Pharmaceutical University, Guangzhou, Guangdong 510006, P.R. China

Received December 19, 2023; Accepted April 22, 2024

DOI: 10.3892/mmr.2024.13253

Abstract. Astragaloside IV (AS-IV) has various pharmacological effects, including antioxidant and immunoregulatory properties, which can improve myasthenia gravis (MG) symptoms. However, the potential mechanism underlying the effects of AS-IV on MG remains to be elucidated. The present study aimed to investigate whether AS-IV has a therapeutic effect on MG and its potential mechanism of action. By subcutaneously immunizing rats with R97-116 peptide, an experimental autoimmune (EA) MG rat model was established. AS-IV (40 or 80 mg/kg/day) treatment was then applied for 28 days after modeling. The results demonstrated that AS-IV significantly ameliorated the weight loss, Lennon score and pathological changes in the gastrocnemius muscle of EAMG rats compared with the model group. Additionally, the levels of acetylcholine receptor antibody (AChR-Ab) were significantly decreased, whereas mitochondrial function [ATPase and cytochrome *c* (Cyt-C) oxidase activities] and ultrastructure were improved in the AS-IV treated rats. Moreover, the mRNA and protein expression levels of phosphatase and tensin homolog-induced putative kinase 1, Parkin, LC3II and Bcl-2, key signaling molecules for mitophagy and apoptosis, were upregulated, whereas the mRNA and protein expression levels of p62, Cyt-C, Bax, caspase 3 and caspase 9 were downregulated following AS-IV intervention. In conclusion, AS-IV may protect against EAMG in a rat model by modulating mitophagy and apoptosis. These findings indicated the potential mechanism underlying the effects of AS-IV on MG and provided novel insights into treatment strategies for MG.

Correspondence to: Professor Tongkai Chen or Professor Yafang Song, Science and Technology Innovation Center, Guangzhou University of Chinese Medicine, 12 Airport Road, Baiyun, Guangzhou, Guangdong 510405, P.R. China
E-mail: chentongkai@gzucm.edu.cn
E-mail: stephanie237@163.com

Abbreviations: AS-IV, astragaloside IV; L-ASIV, low-dose AS-IV; H-ASIV, high-dose AS-IV; MG, myasthenia gravis; EAMG, experimental autoimmune MG; AChR, acetylcholine receptor; Cyt-C, cytochrome *c*; COX, Cyt-C oxidase; PINK1, phosphatase and tensin homolog-induced putative kinase 1; CFA, complete Freund's adjuvant; IFA, incomplete Freund's adjuvant

Key words: AS-IV, MG, mitochondria, mitophagy, apoptosis, skeletal muscle

Introduction

Myasthenia gravis (MG) is a rare chronic autoimmune disease induced by the postsynaptic membrane receptors and autoantibody attack at the neuromuscular junction (NMJ) (1,2). MG manifests as fatigue and muscle weakness, and is associated with diplopia, ptosis and systemic symptoms (3). Previous studies have reported that there are several types of subgroups of MG and that the majority of patients with MG are positive for acetylcholine receptor (AChR) autoantibodies (4-6). At present, there are multiple treatment options available for MG, such as cholinesterase inhibitors, glucocorticoids, immunosuppressants, intravenous immunoglobulins, plasmapheresis and thymectomy, which primarily focus on immunoregulatory mechanisms (7); however, the efficacy of these treatments is limited. Additionally, the numerous side effects of treatments, and the economic burden of therapeutics and surgery further reduce the quality of life of patients. A real-world study showed that after long-term treatment, two-thirds of patients still had moderate to severe symptoms (8). Furthermore, a study performed in Sweden on 1,077 patients showed that ~50% of the patients were 'dissatisfied' with the control of their symptoms (9). MG is a heavy burden on patients worldwide. Although research has previously been performed on MG (10); its pathogenesis has not been fully elucidated and there is an urgent need for novel treatment options.

Mitochondria are the primary organelles that provide energy for cell metabolism. Notably, mitochondrial dysfunction affects human health (11), and an increasing number of studies have revealed that mitochondria are regarded as a therapeutic target for numerous diseases (12,13). Furthermore, it has been identified that mitochondria serve key roles in skeletal muscle function and mitochondrial dysfunction is

related to skeletal muscle damage (14). Previous studies have highlighted the crucial role of normal mitochondrial function in preserving NMJ structure and neurotransmission (15-18); therefore, restoring mitochondrial function holds promise for ameliorating NMJ damage and treating MG (19,20). Previous studies have successfully established an animal model of MG and have performed a series of experimental studies on mitochondria, suggesting that improving mitochondrial function can reduce the symptoms of experimental autoimmune (EA) MG in a rat model (19,21,22).

Mitophagy and apoptosis are the primary means of maintaining mitochondrial homeostasis. Mitophagy is a protective phenomenon that requires the participation of lysosomes, whereas apoptosis is a type of programmed cell death (23). Mitophagy can eliminate the impact of mitochondrial dysfunction, including the excess reactive oxygen species produced, inflammation and oxidative stress (24). Notably, in neurodegenerative diseases typically characterized by the loss of neurons, in which mitophagy and apoptosis are widely involved, abnormalities in synaptic function and instability of the nervous system have been observed (25). Multiple studies have reported that mitophagy and apoptosis serve an important role in diseases, such as spinal muscular atrophy and Duchenne muscular dystrophy (26-29) and regulating mitophagy and apoptosis may exert protective effects on skeletal muscles (30,31). Nevertheless, to the best of our knowledge, no previous studies have elucidated the mechanism underlying aberrant mitophagy and apoptosis in MG. Our unpublished study examined isolated peripheral blood mononuclear cells (PBMC) from patients with MG and observed a decrease in the expression of key signaling molecules involved in promoting mitophagy, along with an increase in the expression of key signaling molecules involved in promoting apoptosis, compared to healthy subjects. Thus, exploring the underlying mechanisms of dysregulated mitophagy and apoptosis in MG is important.

Astragaloside IV (AS-IV) is the primary bioactive component derived from *Astragalus membranaceus* and serves a protective role in various diseases (32). In our previous study, Qiangji Jianli decoction (QJJLD), which is a clinically effective traditional Chinese medicine used for the treatment of MG, was explored and shown to significantly improve gastrocnemius muscle injury in EAMG rats (19). In addition, AS-IV has been identified as the primary component in QJJLD using high-performance liquid chromatography analysis (33); thus, whether AS-IV exerts a similar therapeutic role in MG was assessed in the present study. AS-IV has been reported to exert a potential neuroprotective effect, particularly in neurodegenerative disorders, such as Parkinson's disease (PD) and autoimmune encephalomyelitis (AE) (34). Additionally, traditional Chinese medicines with several multiple active ingredients, such as ginsenoside Rg1 (Rg1), tanshinone IIA (TSA) and AS-IV, which have been shown to exert notable advantages including anti-inflammatory, antioxidant, and anti-apoptotic properties, contributing to neuroprotective effects (35). AS-IV has also been reported to regulate the immune response by regulating the T helper 17/regulatory T cell ratio *in vivo* (36). Furthermore, AS-IV exerts a neuroprotective role by maintaining mitochondrial homeostasis via the regulation of apoptosis and autophagy (37). Notably, AS-IV has been shown to not only regulate mitochondrial dysfunction and inhibit apoptosis of skeletal muscle cells, but also to improve the motor ability of muscles and reverse skeletal muscle injury (38). However, a comprehensive account of the effects of AS-IV on the treatment of MG is, to the best of our knowledge, lacking.

Therefore, in the present study, the protective mechanism of AS-IV in ameliorating EAMG was assessed, with a focus on the regulation of mitophagy and apoptosis, in order to determine the potential mechanism of action and highlight a novel potential therapeutic option for the treatment of MG.

Materials and methods

Animals. A total of 36 female specific pathogen-free (SPF) Lewis rats (weight, 120-140 g; age, 5-6 weeks) were purchased from Charles River Laboratories, Inc. Rats were maintained in SPF conditions at 23±2˚C, 55±5% relative humidity, and under a 12-h light/dark cycle with *ad libitum* access to food and drinking water. Pentobarbital sodium (50 mg/kg) was injected intraperitoneally for anesthesia prior to modeling and repetitive nerve stimulation (RNS) detection to minimize animal pain. All experimental procedures were approved by the Experimental Animal Ethics Committee of Guangzhou University of Chinese Medicine (approval no. 20200509001; Guangzhou, China) and adhered to the National Institutes of Health Guide for the Care and Use of Animals guidelines (39).

Chemicals and reagents. Rat 97-116 peptide of the AChR-α subunit (R97-116, DGDFAIVKFTKVLLDYTGHI) was synthesized by GL Biochem (Shanghai) Ltd. Complete Freund's adjuvant (CFA), incomplete Freund's adjuvant (IFA) and sodium pentobarbital were purchased from MilliporeSigma (cat. nos. F5881, F5506 and P3761, respectively). PBS (cat. no. 10010-023) was purchased from Gibco (Thermo Fisher Scientific, Inc.). An AChR-antibody (AChR-Ab) assay kit (cat. no. ml003131) was obtained from Shanghai Enzyme-linked Biotechnology Co., Ltd. AS-IV (CAS no. 84687-43-4) was purchased from Chengdu Herbpurify Co., Ltd. A Hematoxylin and Eosin (H&E) Staining Kit (cat. no. C0105S) was purchased from Beyotime Institute of Biotechnology. ATPase and cytochrome *c* (Cyt-C) oxidase (COX) assay kits were obtained from Leagene; Beijing Regan Biotechnology Co., Ltd. (cat. nos. DE0045 and DE0031, respectively). Forward and reverse primers were purchased from Generay Biotech Co., Ltd. Phosphatase and tensin homolog-induced putative kinase 1 (PINK1), LC3I/II, Bcl-2, caspase 9 and GAPDH primary antibodies were purchased from Abcam (cat. nos. ab23707, ab128025, ab59348, ab52298 and ab8245, respectively). Parkin, p62, Bax, Cyt-C and caspase 3 primary antibodies were obtained from Cell Signaling Technology, Inc. (cat. nos. 4211, 39749, 2772, 11940 and 9662, respectively).

Establishment of the EAMG animal model. A total of 36 female Lewis rats were acclimated for 1 week in an SPF-level animal room, of which eight were randomly selected as the control group and the remaining 28 rats as the model group. The day of the first immunization was considered day 0. The modeling agent was prepared by mixing 100 μg R97-116

peptide, 0.1 ml CFA and 0.1 ml PBS evenly to form an emulsion. After the preparation of the emulsion mixture, four sites were selected for immunogen injection, including the back, abdomen, and left and right hind foot pads. Each site was injected with 50 μl immune emulsion and the injection site was washed with 75% ethanol. Each rat received a total of 200 μl modeling agent during the first immunization. The second and third immunization boosts were performed on days 30 and 45, respectively, after the first immunization. For these subsequent immunizations, the reagent was prepared by mixing 50 μg R97-116 peptide, 0.1 ml IFA and 0.1 ml PBS, which was injected subcutaneously at the same sites. During the second and third immunization periods, each rat received a total of 200 μl modeling agent each time. During each immunization period, for rats in the control group, the rats were injected subcutaneously with a mixed emulsion of 0.1 ml PBS and 0.1 ml CFA or IFA without R97-116 peptide, and the injection sites and doses were the same as those of the model group rats (40). During the modeling period, the mental state, activity, appetite, stool characteristics and hair luster of each group were recorded daily. The body weight of the rats was measured twice a week, and the Lennon score was recorded. The Lennon score was evaluated using the criteria described previously (41,42), and the assigned Lennon scores were as follows: Grade 0, no weakness; grade 1, fatigability or weakness only observed after exercise; grade 2, clinical signs of weakness present before exercise, including hunched posture or head down; grade 3, severe muscle weakness with dyspnea/apnea or moribund state; grade 4, death. Intermediate signs in rats were categorized into grades 0.5, 1.5, 2.5 or 3.5, accordingly. The model was evaluated 1 week after the third immunization. Rats in both groups undergoing experimental treatment were euthanized at day 80 or when they reached a humane endpoint, such as self-harming behavior, severe weight loss of 20%, compromised breathing or lack of response to external stimuli. Sodium pentobarbital (150 mg/kg) was injected intraperitoneally to euthanize the rats. Death was confirmed by monitoring the cessation of breathing and heartbeat, and pupil dilation. Throughout the course of the experiment, only one rat in the model group reached the predefined humane endpoints at the day 49.

RNS. After anesthesia, the rats in the model group were immobilized. Stimulating electrodes of the electrophysiological recorder (cat. no. PL3516; PowerLab; ADInstruments, Ltd.) were placed near the sciatic nerve in the gastrocnemius muscle, recording electrodes were subcutaneously implanted in the medial head of the gastrocnemius muscle and Achilles tendon on the same side, and reference electrodes were subcutaneously implanted in the abdomen (43). All electrodes received 10 pulses of 5 Hz electrical stimulation, and the percentage change of the first and fifth action potentials was measured. A positive result was defined as an attenuation rate of >10%.

Detection of AChR-Ab. On day 7 after modeling completion, rats were anesthetized with an intraperitoneal injection of 30 mg/kg pentobarbital sodium. Subsequently, a single blood sample of 0.2-0.4 ml was collected from the orbital venous plexus of each rat. Additionally, upon completion of the entire experiment and euthanasia of the rats, a blood sample of 0.8-1 ml was collected once from the abdominal aorta. The collected blood samples were placed in centrifuge tubes for 30 min and left to stand. The tubes were then centrifuged at 1,500 x g for 10 min at 4˚C, and the supernatant was collected and stored at -80˚C. The AChR-Ab levels in the rats were measured in the serum using the aforementioned specific ELISA kit.

Drug intervention. Following three separate immunizations, 24 of the 28 rats in the model group were successfully modeled, and the rate at which the EAMG rat model was successfully established was 85.71%. The model group was randomly divided into three subgroups: Model group, low-dose AS-IV (L-ASIV) group and high-dose AS-IV (H-ASIV) group (n=8 rats/group). The rats in the L-ASIV and H-ASIV groups were treated with 40 and 80 mg/kg/day AS-IV by gavage, respectively (44-46). The control and model groups were administered equal volumes of saline by gavage, and the gavage volume was calculated according to the principle of 1 ml/kg body weight. During the four-week Drug intervention, rats in each group were administered via gavage once a day, following the respective treatment method. The rats were fasted for 24 h after the last administration. Sodium pentobarbital (150 mg/kg) was injected intraperitoneally for euthanasia, and death was confirmed by monitoring the cessation of breathing and heartbeat, and pupil dilation (47).

H&E staining. After the rats were sacrificed, the gastrocnemius muscle tissue was immediately removed and fixed overnight at room temperature in 4% paraformaldehyde and was then embedded in conventional paraffin. The tissues were cut into 4-μm sections, which were stained with 100% hematoxylin solution at room temperature for 2 min and were then differentiated in 1% hydrochloric acid ethanol for several seconds. After rinsing with water and dehydrating in a series of increasing concentrations of ethanol, the sections were stained with 100% eosin solution at room temperature for 1 min. The sections were then placed in xylene until they became transparent and were mounted with neutral gum. Images of the sections from each group were captured under an optical microscope at a magnification of x400 (Olympus BX53; Olympus Corporation).

Transmission electron microscopy (TEM). After 4 weeks of treatment, gastrocnemius muscle samples were cut to a volume of 1 mm^3 and fixed with 2.5% glutaraldehyde at 4˚C for 2-6 h. The sections were then rinsed in phosphoric acid buffer solution for 30 min (repeated six times), fixed with 1% osmic acid at 4˚C for 1.5-2 h, and rinsed again in phosphoric acid buffer solution for 10 min (repeated three times). After dehydration in a series of increasing concentrations of ethanol, the tissue samples were embedded in epoxy resin monomer overnight at 37˚C. An ultramicrotome (RM2016; Leica Microsystems GmbH) was used for sectioning (60 nm), and the samples were then stained with uranium dioxide acetate at room temperature for 12 min and with lead citrate at room temperature for 8 min. Finally, the ultrastructure was observed using TEM (Jem-1400; JEOL, Ltd.).

Table I. Primers used for reverse transcription-quantitative PCR.

Gene	Forward primer, 5'-3'	Reverse primer, 3'-5'
PINK1	CATGGCTTTGGATGGAGAGT	TGGGAGTTTGCTCTTCAAGG
Parkin	CTGGCAGTCATTCTGGACAC	CTCTCCACTCATCCGGTTTG
p62	CCAGCACAGGCACAGAAGATAAGAG	TCCCACCGACTCCAAGGCTATC
LC3II	TCGCCGACCGCTGTAAGGAG	CGCCGGATGATCTTGACCAACTC
Caspase 3	TCTACCGCACCCGGTTACTA	CGTACAGTTTCAGCATGGCG
Caspase 9	CTGAGCCAGATGCTGTCCCATA	GACACCATCCAAGGTCTCGATGTA
Bcl-2	TCCTTCCAGCCTGAGAGCAACC	CGACGGTAGCGACGAGAGAAGT
Bax	CCCCCGAGAGGTCTTTTTCCG	GGGCCTTGAGCACCAGTTTGC
Cyt-C	GCTAAACACCAGGACGGAACT	CCACTCCCAATCAGGCATGAAC
GAPDH	TGATTCTACCCACGGCAAGTT	TGATGGGTTTCCCATTGATGA

PINK1, phosphatase and tensin homolog-induced putative kinase 1; Cyt-C, cytochrome *c*.

ATPase staining. An ATPase staining kit was used for ATPase staining. Fresh gastrocnemius muscle tissues were embedded in a frozen section embedding agent and frozen at -20˚C for further processing. The embedded tissues were then cut into 6 μm frozen sections and placed in distilled water. The sections were incubated in calcium salt solution at 37˚C for 5 min, then incubated with ATPase incubation solution at 37˚C for 40 min, followed by washing with distilled water. Subsequently, the sections were immersed in cobalt nitrate solution at 37˚C for 5 min and then in distilled water. They were then fixed with 4% neutral formalin at room temperature for 2 min and rinsed with running water for 2 min. The sections were placed in a prepared sulfide working solution and incubated for 2 min. After washing with water, the sections were mounted with glycerol gelatin onto slides. Images were captured under a fluorescence microscope (Olympus Corporation) at x50 magnification and the average optical density values of the images were calculated using ImagePro Plus (version 6.0; Media Cybernetics, Inc.).

Assay of COX activity. The frozen sections of gastrocnemius muscle of rats were dehydrated in an increasing concentration gradient of ethanol (5 min at each concentration). The frozen sections were then soaked in xylene solution twice (10 min each), the excess liquid on the slide was removed with absorbent paper and the slides were sealed with neutral gum. Subsequently, DAB solution was added to the frozen sections and incubated at 37˚C in the dark for 90 min, before the sections were washed with distilled water three times (3 sec each). The staining of frozen sections was observed under an optical microscope (EcliPse E100; Nikon Corporation).

Reverse transcription-quantitative (RT-q)PCR. Total RNA was obtained from the gastrocnemius muscle tissue samples of rats using TRNzol-A$^+$ (Tiangen Biotech Co., Ltd.). cDNA was synthesized by RT using a PrimeScript™ RT MasterMix Kit (Takara Bio, Inc.). The expression of target genes was quantified by qPCR with TB Green™ Premix Ex Taq™ II (Takara Bio, Inc.) using a CFX96 Real-Time PCR System (Bio-Rad Laboratories, Inc.). The RT temperature protocol was 37˚C for 15 min and 85˚C for 5 sec. The thermocycling conditions for qPCR amplification were 95˚C for 30 sec for initial denaturation; followed by 40 cycles of 95˚C for 5 sec and 60˚C for 30 sec and extension at 72˚C for 20 sec, followed by a final extension at 72˚C for 5 min. The primer sequences of all target genes are shown in Table I. Relative quantification was performed using the $2^{-\Delta\Delta Cq}$ method (48), with GAPDH as the reference gene.

Western blot analysis. Total protein was extracted from the gastrocnemius muscle tissues with RIPA lysis buffer (cat. no. KGP2100; Nanjing KeyGen Biotech Co., Ltd.) on ice, then centrifuged at 10,000 x g for 15 min at 4˚C to collect the supernatants. A bicinchoninic acid assay (cat. no. KGP902; Nanjing KeyGen Biotech Co., Ltd.) was used to measure the protein concentration. Equal amounts of protein (30 μg) were loaded on 10 and 12% SDS-gels, resolved using SDS-PAGE and subsequently transferred to a PVDF membrane. Membranes were blocked using 5% skimmed milk (cat. no. 232100; Difco; BD Biosciences) at room temperature for 1 h and were then incubated overnight with primary antibodies at 4˚C with agitation. The following primary antibodies were used: Anti-PINK1 (1:1,000), anti-LC3A/B (1:1,000), anti-Bcl-2 (1:1,000), anti-caspase 9 (1:1,000), anti-GAPDH (1:5,000), anti-Parkin (1:1,000), anti-SQSTM1/p62 (1:1,000), anti-caspase 3 (1:1,000), anti-Bax (1:1,000) and anti-Cyt-C (1:1,000). Subsequently, the membranes were washed and incubated with the secondary HRP-conjugated Goat Anti-Rabbit IgG antibody (1:3,000; cat. no. CW0103S; CW Biosciences) or Goat Anti-Mouse IgG antibody (1:3,000; cat. no. CW0102S; CW Biosciences) at room temperature for 1 h, and the protein bands were observed using a Western ECL Substrate kit (cat. no. 170-5061; Bio-Rad Laboratories, Inc.). Signals were visualized using a gel imaging system (Chemi Doc XRS+; Bio-Rad Laboratories, Inc.), and Image Lab software (version 6.0; Bio-Rad Laboratories, Inc.) was used for densitometric analysis. All experiments were repeated independently at least three times.

Statistical analysis. All data are presented as the mean ± standard deviation or as median and IQR. Graphs were

generated using GraphPad Prism version 9 (Dotmatics). SPSS version 22.0 (IBM Corp.) was used for data processing. Statistical differences between two groups were determined using unpaired Student's t-test. Comparisons among more than two groups were carried out using one-way analysis of variance, followed by the Tukey's post hoc test. The nonparametric Mann-Whitney U test or Kruskal-Wallis test followed by Dunn's multiple comparisons test were used to analyze the Lennon score data. P<0.05 was considered to indicate a statistically significant difference.

Results

Construction of the EAMG rat model. Lewis rats were immunized by subcutaneously injecting peptide R97-116 as an antigen to induce EAMG (Fig. 1A); ~20 days after the first immunization, the majority of the rats in the model group exhibited a decrease in water and food consumption, weight loss and muscle weakness (increased Lennon score), compared with the rats in the control group (Fig. 1B and C). After the third booster immunization, one rat was sacrificed due to reaching humane endpoints, and the rest of the model group rats exhibited decreased activity, low and weak cries, dull and yellow fur, marked weight loss and muscle weakness (increased Lennon score); the differences between the model group and the control group were statistically significant (both P<0.01; Fig. 1B and C). After modeling, the rats were anesthetized and the changes in the response to RNS in each group were measured using electromyography. The attenuation of the first action potential amplitude and the fifth action potential amplitude of model rats was >10%, and the differences between the model group and the control group was statistically significant (P<0.01; Fig. 1D and E). ELISA was used to detect the levels of AChR-Ab in the rats. Compared with in the control group, the AChR-Ab content in the serum of rats in the model group was significantly increased (P<0.01; Fig. 1F).

Effects of AS-IV on EAMG rats. After modeling, the different groups were treated with normal saline or AS-IV (Fig. 2A) for 4 weeks. In the model group, the weight and muscle strength of rats continued to decline after treatment with normal saline. After 4 weeks of treatment, compared with in the model group, the average weight of EAMG rats in the H-ASIV and L-ASIV groups significantly increased (P<0.01; Fig. 2B). The Lennon score also significantly decreased, indicating improved MG symptoms (P<0.01; Fig. 2C). Electromyography (EMG) was then used to observe the changes in the response to RNS in each group, and the levels of AChR-Ab in the blood samples from each group were measured. There was no significant change in the EMG amplitude in the control group, but the EMG amplitude attenuation rate in the model group was >10% compared with that in the control group (P<0.01; Fig. 2D and E). By contrast, the RNS amplitude attenuation of rats in the H-ASIV and L-ASIV groups recovered and was significantly reduced compared with that in the model group (P<0.01 and P<0.05, respectively; Fig. 2D and E). Compared with in the control group, the AChR-Ab levels of rats in the model group were significantly increased (P<0.01; Fig. 2F). By contrast, the AChR-Ab levels in the blood samples from the H-ASIV and L-ASIV groups were significantly reduced compared with those in the model group (P<0.01 and P<0.05, respectively; Fig. 2F). Taken together, these results suggested that AS-IV can improve the symptoms of EAMG in a rat model.

Effects of AS-IV on the morphology and ultrastructure of gastrocnemius muscle. The muscle fibers of rats in the control group were tight, normal and orderly, with nuclei evenly distributed at the edge of the fibers (Fig. 3A). In the model group, muscle fiber atrophy, widening of the spaces between fibers, edema and degeneration, connective tissue formation and mass inflammatory cell infiltration were observed. Following treatment with AS-IV, both the low and high dose groups showed varying degrees of improvement, especially at the higher dose, and the muscle fiber morphology was similar to that observed in the control group (Fig. 3A).

TEM was used to observe changes in the muscle fiber arrangement and mitochondrial ultrastructure in the gastrocnemius muscle tissue of rats (Fig. 3B). In the control group, the gastrocnemius muscle tissue was tight, the muscle fibers were arranged in an orderly manner, the mitochondrial structure was complete and clear, and the cristae were visible. In the model group, most muscle fibers appeared broken, the number of mitochondria was notably reduced, and the mitochondrial structure was incomplete. In the L-ASIV group, the muscle fibers of rats appeared severely broken, some mitochondria were swollen, vacuolated and showed aggregation, but the number of mitochondria was higher than that in the model group. In the H-ASIV group, fewer broken muscle fibers were observed compared with in the model group, with visible cristae and complete mitochondrial structure. In addition, autophagosomes in the gastrocnemius muscle tissue were observed using TEM. In the model group, no autophagosomes were observed under TEM, whereas AS-IV treatment markedly increased the number of autophagosomes (Fig. 3B). Briefly, these results indicated that AS-IV notably improved the morphology of the gastrocnemius muscle, the ultrastructure of mitochondria and the dysregulated mitophagy in rats.

Effects of AS-IV on ATPase activity in gastrocnemius muscle. ATPase hydrolyzes ATP into ADP and phosphate, and releases energy for almost all essential cellular processes (49). In the gastrocnemius muscle of control rats, active site of ATPase staining is brown and black, and positive expression of ATPase was detected (Fig. 4A and B). In the model group, the intensity of staining was low and ATPase expression was significantly reduced compared with that in the control group, suggesting that ATPase activity was decreased (P<0.01). After treatment with AS-IV, the intensity of staining was higher, expression increased and ATPase activity was significantly increased in H-ASIV and L-ASIV groups compared with that in the model group (P<0.01 and P<0.05, respectively; Fig. 4A and B). In summary, these results suggested that AS-IV can improve ATPase activity and restore mitochondrial function.

Effect of AS-IV on COX activity in the skeletal muscle of EAMG rats. COX is an enzyme present in mitochondria, which serves a crucial role in maintaining the normal structure and function of mitochondria (50). To evaluate COX activity, an optical microscope was used to observe the differences in

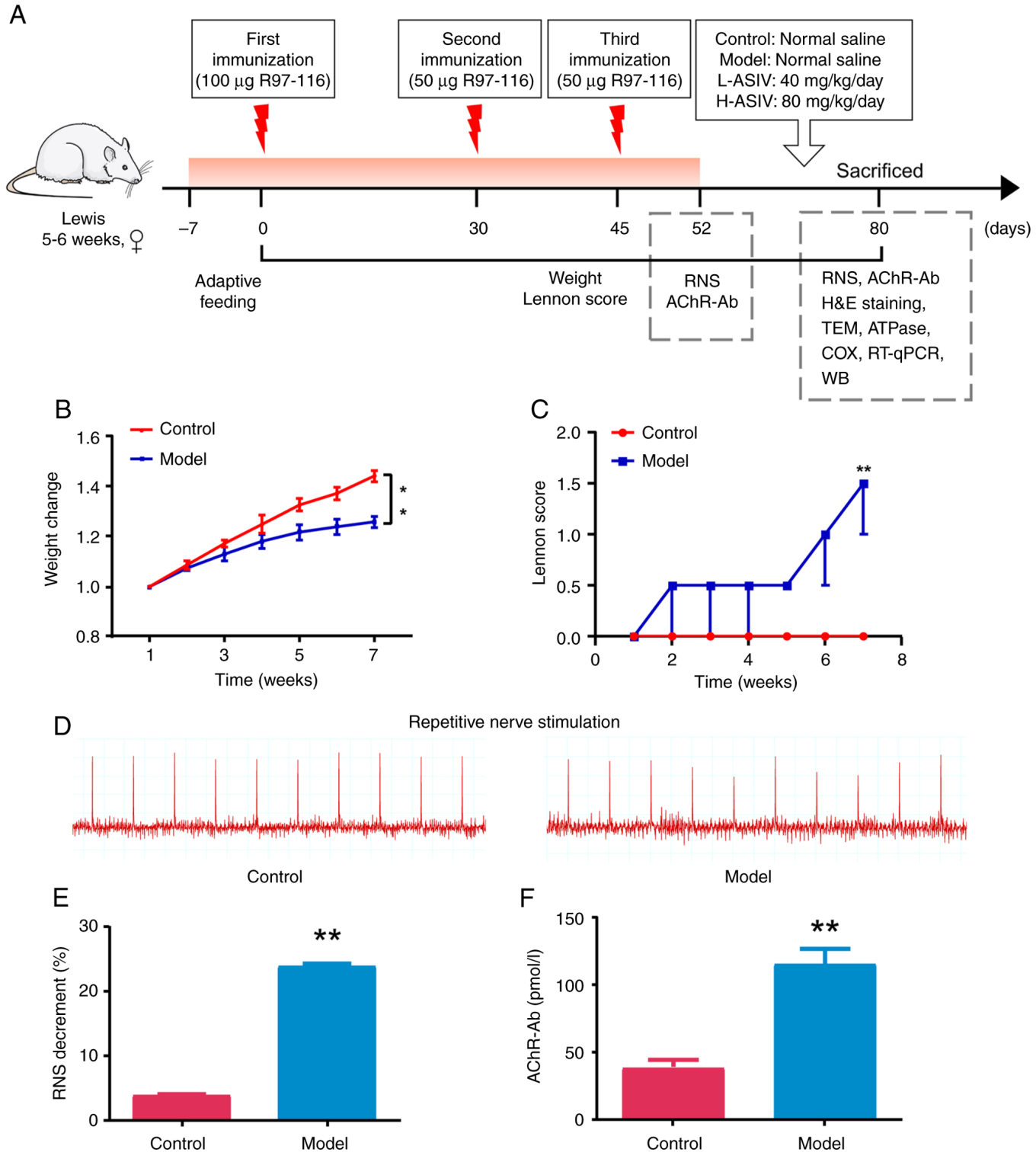

Figure 1. Construction and evaluation of the EAMG rat model. (A) Experimental protocol for treatment of EAMG rats with AS-IV. (B) Weight change rate after modeling. (C) Changes in Lennon score in different groups. (D) Degree of electrical attenuation was detected by RNS in both the control and model groups at 1 week after the last immunization. (E) Quantitative diagram of the RNS analysis. The amplitude attenuation of the first and fifth action potentials in the model group decreased by >10%, which was considered positive. (F) Rat serum samples were collected at the indicated time points after disease induction and were analyzed by ELISA for rat AChR-Ab. **P<0.01 vs. control. AChR-Ab, acetylcholine receptor antibody; AS-IV, astragaloside IV; COX, cytochrome *c* oxidase; EAMG, experimental autoimmune myasthenia gravis; H-ASIV, high-dose AS-IV; H&E, hematoxylin and eosin; L-ASIV, low-dose AS-IV; RNS, repetitive nerve stimulation; RT-qPCR, reverse transcription-quantitative PCR; TEM, transmission electron microscopy; WB, western blotting.

COX staining in the gastrocnemius muscle tissues after intragastric treatment for 4 weeks. COX staining of frozen sections of gastrocnemius tissue in the control group showed that the myofibrils were polygonal and of equal size; the color at active part of COX staining was indicated by brown grain precipitation. Compared with in the control group, COX activity in the model group was lower with lighter brown grain precipitation in most positively stained areas, and irregularities in the size

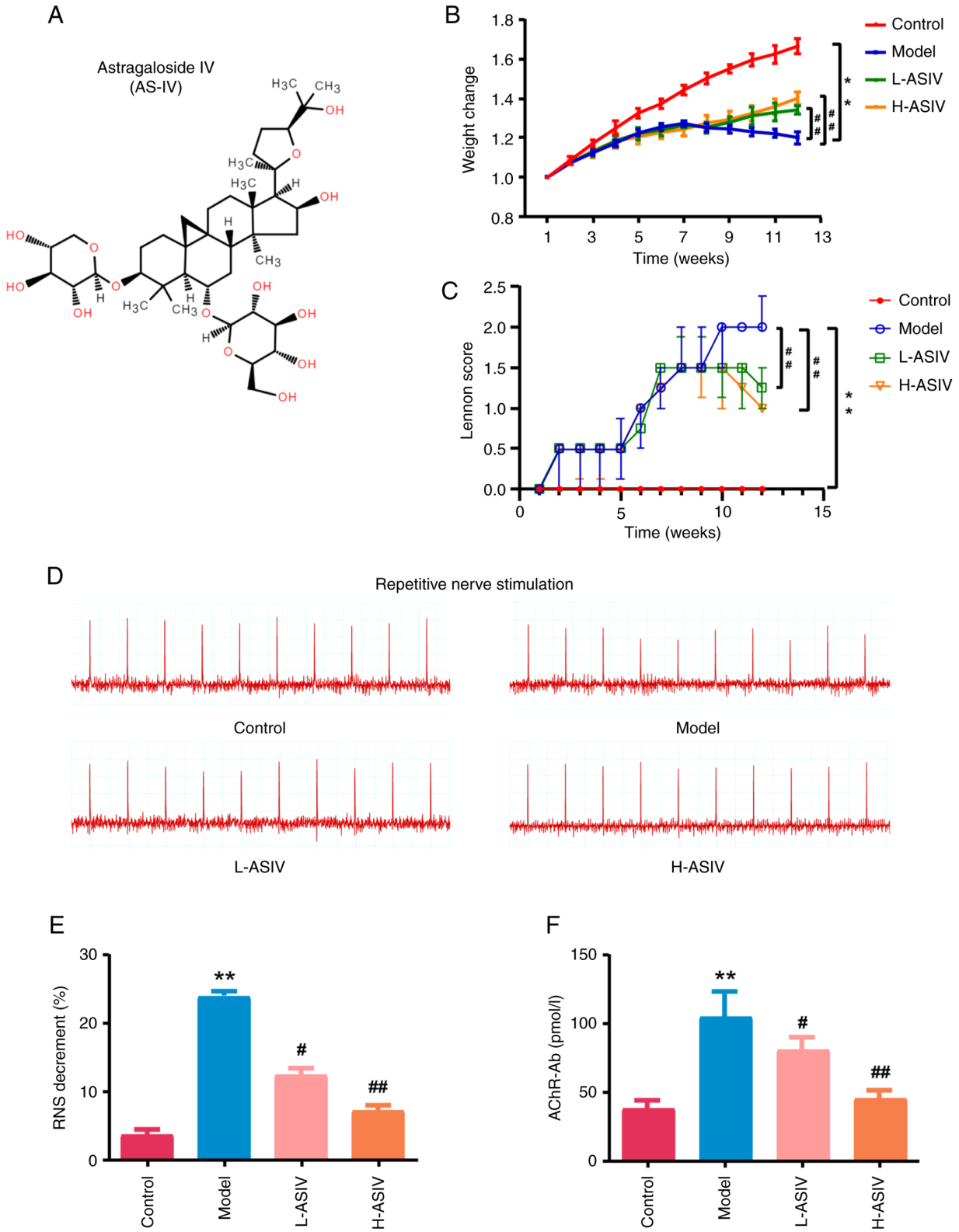

Figure 2. Therapeutic effect of AS-IV on experimental autoimmune myasthenia gravis rats. After modeling, the different groups were treated with normal saline and AS-IV for 4 weeks. (A) Chemical structure of AS-IV. (B) Change of average body weight ratio before and after treatment. (C) Changes in Lennon scores in different groups; n=8. (D). Changes of RNS in each group after treatment with saline or AS-IV. (E) Quantitative diagram of the repetitive nerve stimulation analysis; n=8. (F) Concentration of AChR-Ab in rat serum was measured by ELISA; n=8. **P<0.01 vs. control group; $^{\#}$P<0.05, $^{\#\#}$P<0.01 vs. model group. AChR-Ab, acetylcholine receptor antibody; AS-IV, astragaloside IV; H-ASIV, high-dose AS-IV; L-ASIV, low-dose AS-IV.

and shape of myofibrils was observed (Fig. 4C). In the L-ASIV group, COX activity was low and the positively stained area showed a lighter brown grain precipitation, accompanied with the myofibrils exhibited irregular shapes. There was a notable difference in the H-ASIV group when compared with the model group, which presented regularly shaped myofibrils

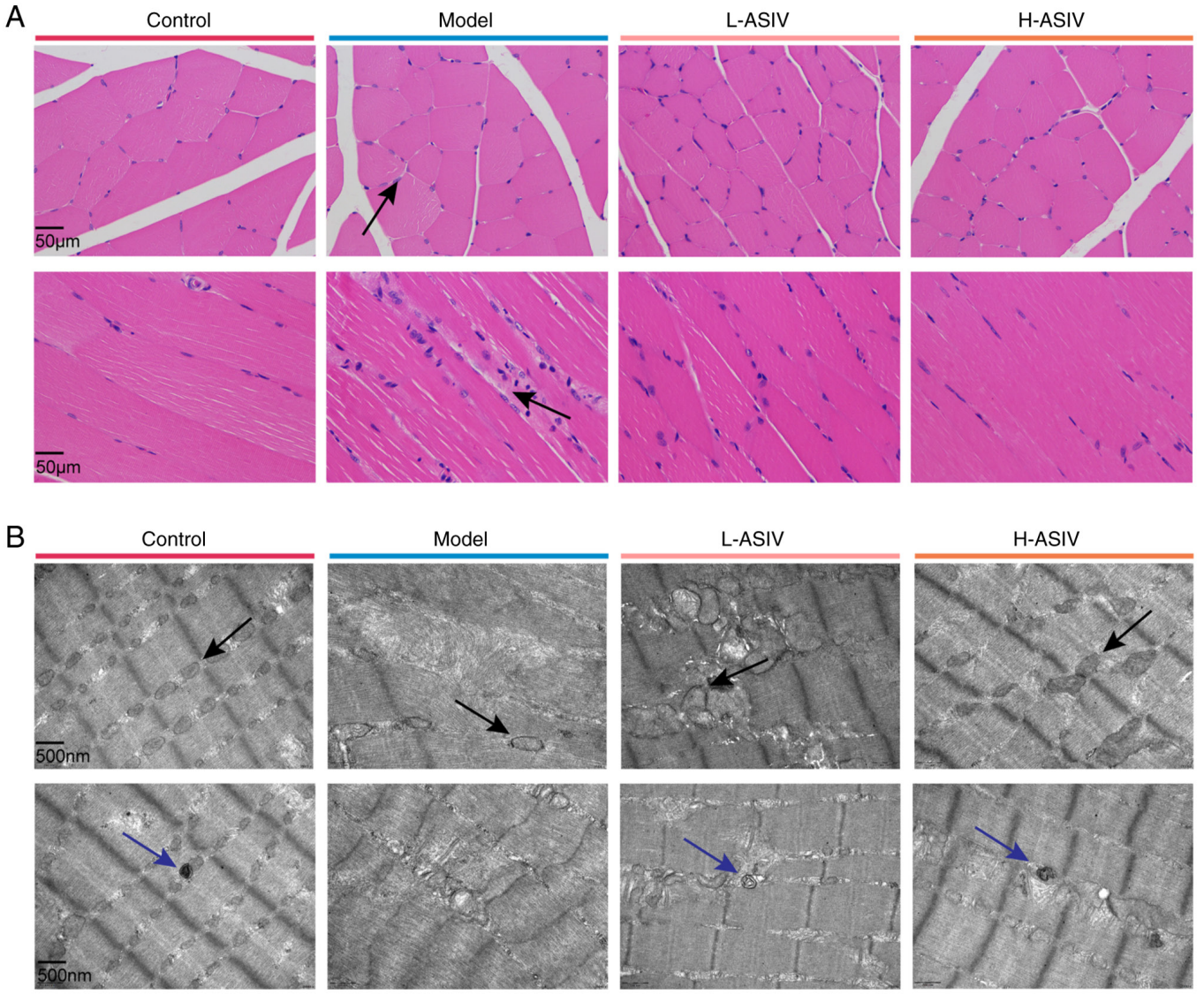

Figure 3. Effects of AS-IV on histological morphology and mitochondrial ultrastructure of the rat gastrocnemius muscle in each group. (A) Hematoxylin and eosin staining to characterize the internal structure of the gastrocnemius muscle fiber of rats in each group. Representative images of gastrocnemius muscle cross-sections (upper images) and longitudinal sections (lower images) were captured by microscopy (scale bar, 50 μm). The lesion area is indicated by black arrows. (B) Transmission electron microscopy observations of the arrangement of muscle fibers and the ultrastructure of mitochondria in the gastrocnemius muscle of rats in each group. Mitochondria with a relatively complete structure are labeled with black arrows, while the blue arrows indicate autophagosomes (scale bar, 500 nm). AS-IV, astragaloside IV; H-ASIV, high-dose AS-IV; L-ASIV, low-dose AS-IV.

and more intense staining (Fig. 4C). Compared with in the control group, the intensity of distribution (IOD)/area of COX activity in the model group was significantly reduced (P<0.05; Fig. 4D). By contrast, compared with in the model group, in the H-ASIV group, the IOD/area of COX activity was significantly increased (P<0.05; Fig. 4D). Therefore, these results suggested that AS-IV improved COX activity to preserve mitochondrial structure and function.

AS-IV promotes PINK1/Parkin-mediated mitophagy in the skeletal muscle of EAMG rats. To further understand the mechanism of action of AS-IV, its effects on the mRNA and protein expression levels of members of the mitophagy-related signaling pathway were determined. As shown in Fig. 5A-D, compared with those in the control group, the mRNA expression levels of PINK1, Parkin and LC3II in the model group were decreased, whereas the mRNA expression levels of p62 were increased (all P<0.01). Compared with in the model group, the difference in the mRNA expression levels of PINK1, Parkin, p62 and LC3II in the L-ASIV group was not significant, whereas the mRNA expression levels of PINK1, Parkin and LC3II were significantly increased in the H-ASIV group (P<0.05 or P<0.01). Additionally, the mRNA expression levels of p62 were significantly decreased in the H-ASIV group (P<0.01).

The protein expression levels of the aforementioned molecules were further assessed using western blotting following AS-IV treatment. As shown in Fig. 6A-E, the protein expression levels of PINK1, Parkin, and LC3II/I in the model group were significantly lower than those in the control group, whereas the protein expression levels of p62 were significantly increased (all P<0.01). After treatment with AS-IV, compared with those in the model group, the protein expression levels of PINK1, Parkin, and LC3II/I in the H-ASIV group were

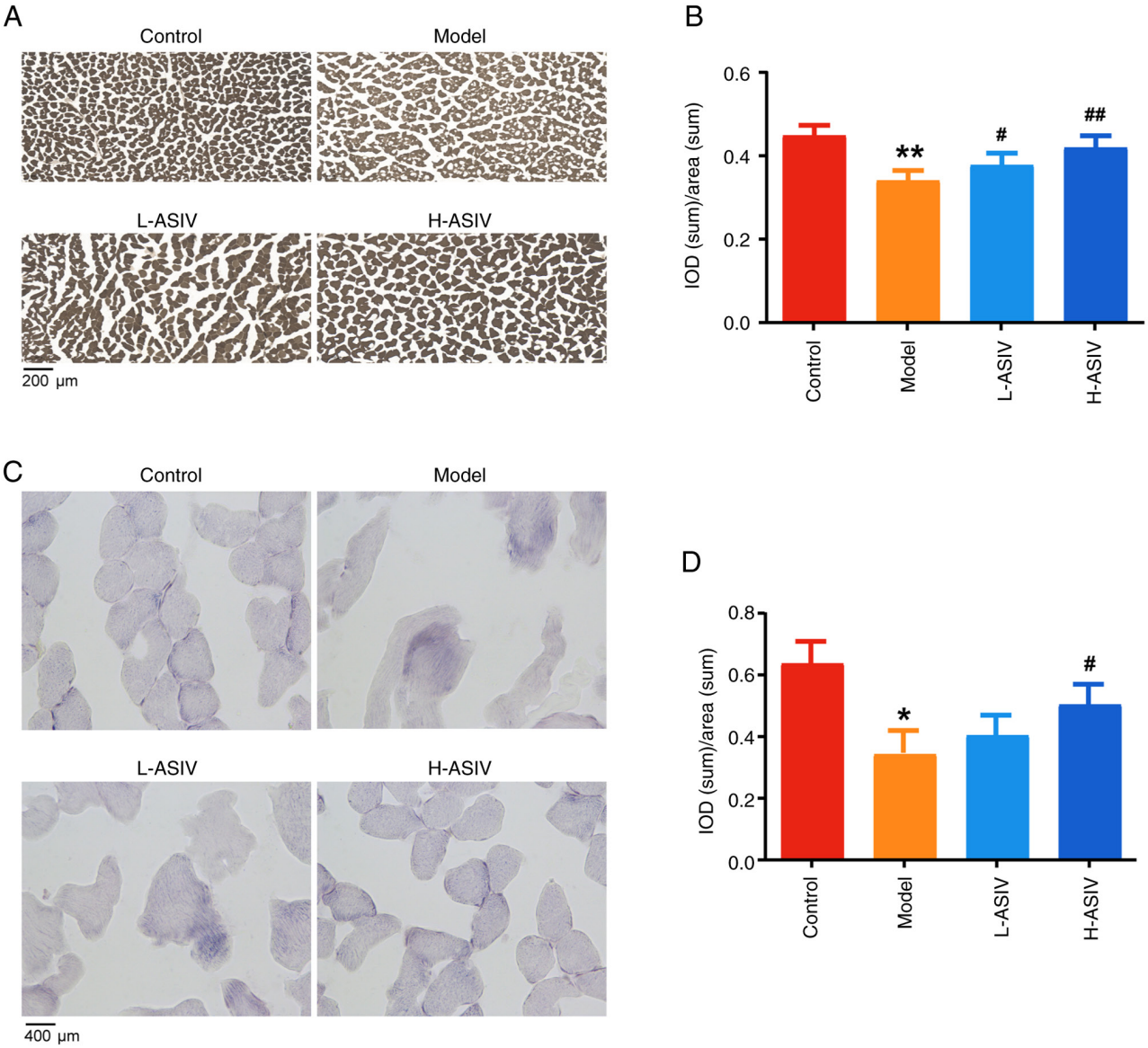

Figure 4. Protective effect of AS-IV on structure and function of mitochondria in the gastrocnemius muscle of experimental autoimmune myasthenia gravis rats. ATPase and COX activities in the gastrocnemius muscle of rats from each group. (A) Effect of AS-IV on ATPase staining. (B) Quantification of the IOD of ATPase in rats from each group; n=8. (C) Effect of AS-IV on COX staining. (D) Quantification of the IOD of COX in rats from each group; n=8. *P<0.05, **P<0.01 vs. control group; $^{\#}$P<0.05, $^{\#\#}$P<0.01 vs. model group. AS-IV, astragaloside IV; COX, cytochrome *c* oxidase; H-ASIV, high-dose AS-IV; IOD, intensity of distribution; L-ASIV, low-dose AS-IV.

significantly higher, and the expression levels of p62 were significantly decreased (P<0.05 or P<0.01). By contrast, there was no significant difference in the protein expression levels in the L-ASIV group. Taken together, these results suggested that AS-IV can promote PINK1/Parkin-mediated mitophagy in the skeletal muscle of EAMG rats.

AS-IV ameliorate expression of mitochondrial apoptosis-associated proteins/genes in the skeletal muscle of EAMG rats. Subsequently, we conducted further investigations to observe the impact of AS-IV on the mRNA and protein expression levels of mitochondrial apoptosis-related signaling pathway components. As shown in Fig. 7A-E, the mRNA expression levels of Bax, Cyt-C, caspase 3 and caspase 9 were significantly higher (P<0.01), and the mRNA expression levels of Bcl-2 were significantly lower (P<0.01), in the skeletal muscle tissues of the model group compared with in the control group. After 4 weeks of AS-IV treatment, the expression levels of Cyt-C, Bax, caspase 3 and caspase 9 were significantly lower in the L-ASIV and H-ASIV groups than those in the model group (all P<0.01; except for Cyt-C in the L-ASIV group, P<0.05). By contrast, Bcl-2 expression in the H-ASIV and L-ASIV groups was significantly higher than that in the model group (P<0.01).

Western blotting was used to detect the protein expression levels of the aforementioned genes. As shown in Fig. 8A-F, the protein expression levels of Cyt-C, Bax, caspase 3 and caspase 9 were significantly higher (all P<0.01), and the expression levels of Bcl-2 were significantly lower (P<0.01) in the skeletal muscle of the model group compared with those in the control group. After 4 weeks of AS-IV treatment, the expression levels of Cyt-C, Bax, caspase 3 and caspase 9 in the H-ASIV and

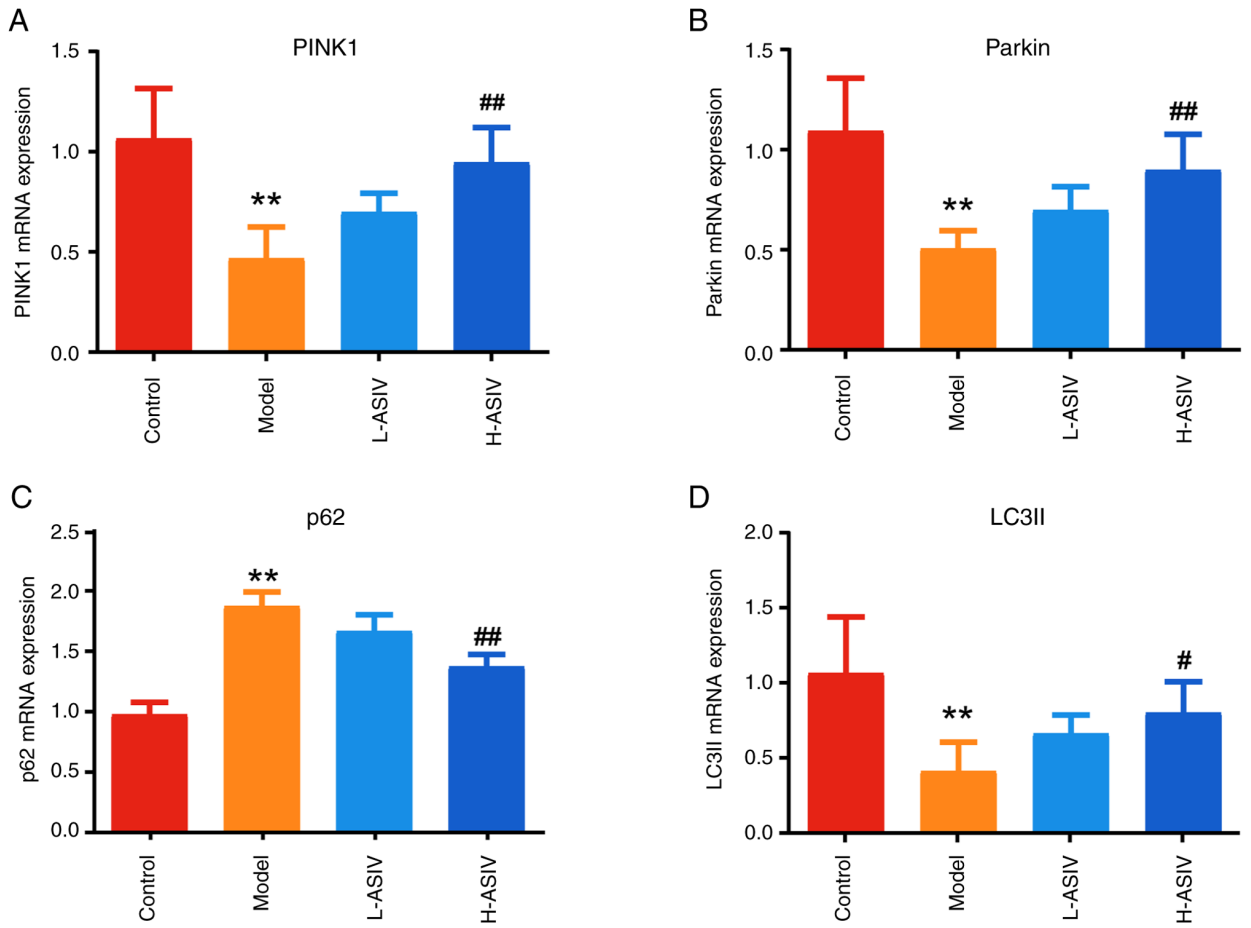

Figure 5. Effects of AS-IV on mRNA expression related to mitophagy. Reverse transcription-quantitative PCR was used to analyze mRNA expression. Effect of AS-IV on the mRNA expression levels of (A) PINK1, (B) Parkin, (C) p62 and (D) LC3II; n=8. **P<0.01 vs. control group; $^{\#}$P<0.05, $^{\#\#}$P<0.01 vs. model group. AS-IV, astragaloside IV; H-ASIV, high-dose AS-IV; L-ASIV, low-dose AS-IV; PINK1, phosphatase and tensin homolog-induced putative kinase 1.

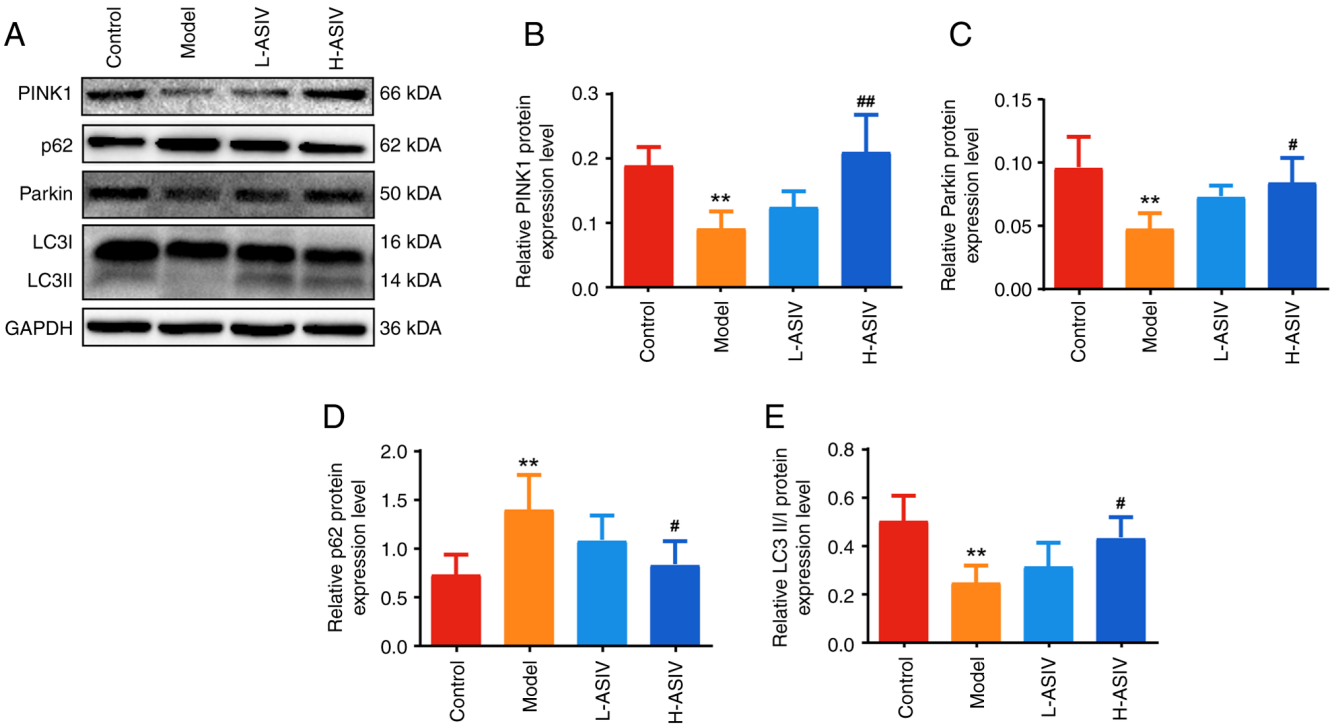

Figure 6. Effects of AS-IV on the expression of proteins related to mitophagy. (A) Western blotting was used to analyze protein expression. Effect of AS-IV on the protein expression levels of (B) PINK1, (C) Parkin, (D) p62 and (E) LC3II/I; n=8. **P<0.01 vs. control group; $^{\#}$P<0.05, $^{\#\#}$P<0.01 vs. model group. AS-IV, astragaloside IV; H-ASIV, high-dose AS-IV; L-ASIV, low-dose AS-IV; PINK1, phosphatase and tensin homolog-induced putative kinase 1.

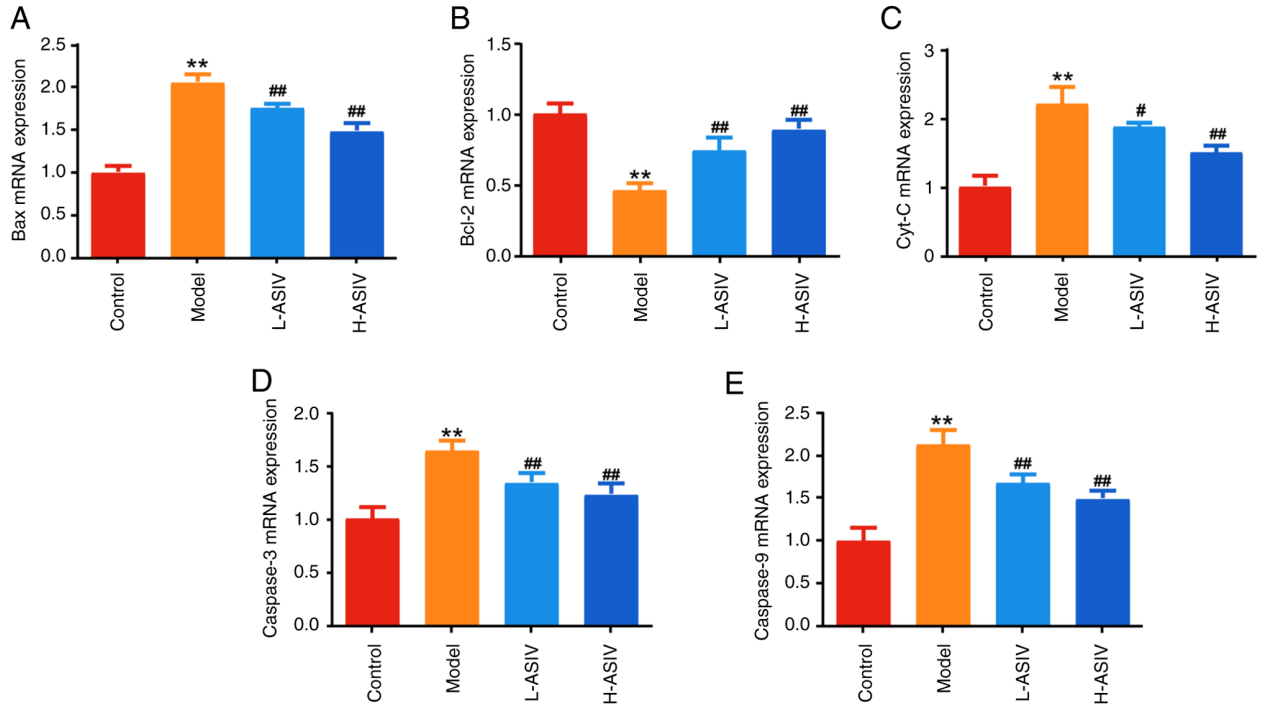

Figure 7. Effects of AS-IV on mRNA expression related to mitochondrial apoptosis. Reverse transcription-quantitative PCR was used to analyze mRNA expression. Effect of AS-IV on the mRNA expression levels of (A) Bax, (B) Bcl-2, (C) Cyt-C, (D) caspase 3 and (E) caspase 9; n=8. **P<0.01 vs. control group; $^{\#}$P<0.05, $^{\#\#}$P<0.01 vs. model group. AS-IV, astragaloside IV; Cyt-C, cytochrome *c*; H-ASIV, high-dose AS-IV; L-ASIV, low-dose AS-IV.

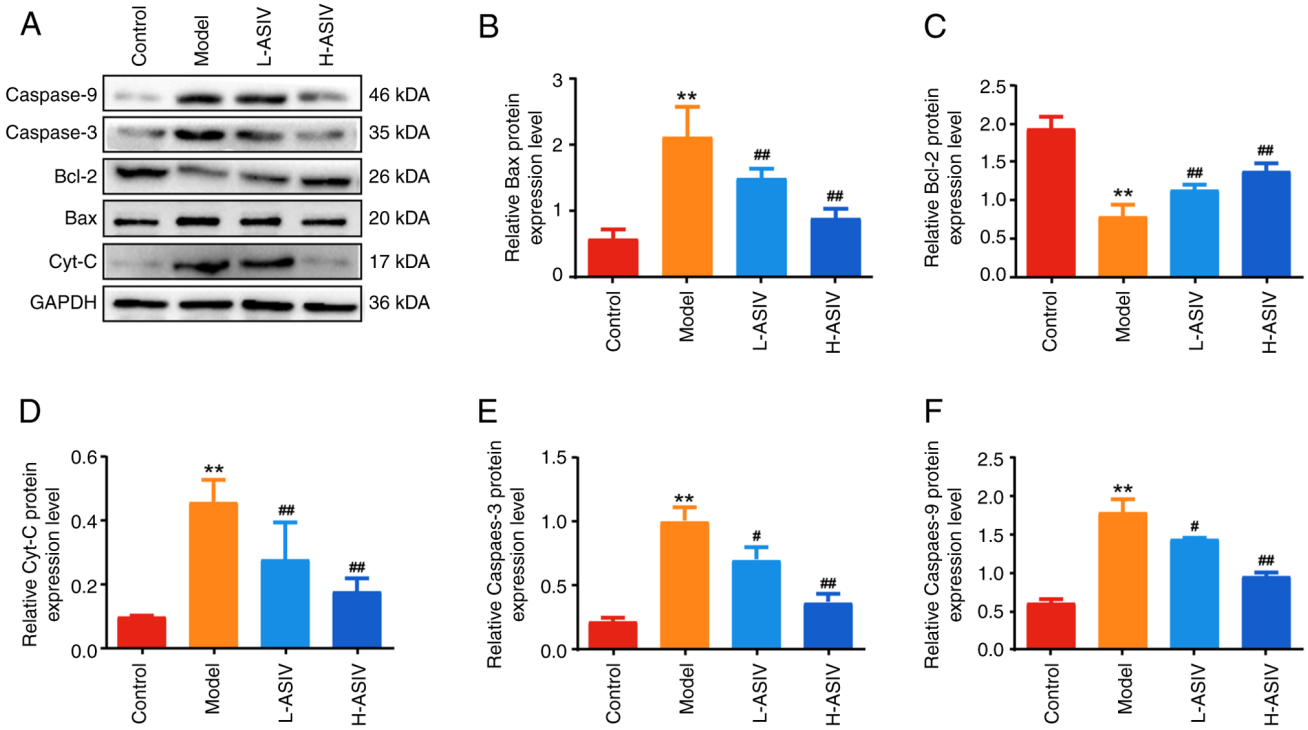

Figure 8. Effects of AS-IV on the expression of proteins related to mitochondrial apoptosis. (A) Western blotting was used to analyze protein expression. Effect of AS-IV on the protein expression levels of (B) Bax, (C) Bcl-2, (D) Cyt-C, (E) caspase 3 and (F) caspase 9; n=8. **P<0.01 vs. control group; $^{\#}$P<0.05, $^{\#\#}$P<0.01 vs. model group. AS-IV, astragaloside IV; Cyt-C, cytochrome *c*; H-ASIV, high-dose AS-IV; L-ASIV, low-dose AS-IV.

L-ASIV groups were significantly lower than those in the model group (all P<0.01; except for caspase 3 and 9 in the L-ASIV group, P<0.05). In addition, the protein expression levels of Bcl-2 in the H-ASIV and L-ASIV groups were significantly higher than those in the model group (P<0.01). In summary, these results indicated that AS-IV can ameliorate the expression of mitochondrial apoptosis-associated proteins/genes in the skeletal muscle of EAMG rats.

Discussion

AS-IV has been shown to exert pharmacological effects, such as antioxidant, anti-inflammatory, anti-apoptotic and immune-enhancing activities. Previous studies have also confirmed that AS-IV alleviates neuron and Schwann cell damage and improves neural functional deficits (51-53), which significantly improves neurodegenerative diseases, such as Alzheimer's disease (AD) and PD (54). Moreover, AS-IV has demonstrated favorable therapeutic effects on neuromuscular disorders, such as amyotrophic lateral sclerosis (ALS), which has been attributed to its ability to ameliorate inflammatory responses and neurotransmission (29,34,55,56). Since MG is a representative neuromuscular disease (57), it is reasonable to speculate that AS-IV may offer therapeutic effects in its management. In the present study, an EAMG rat model was established, and a reduction in body weight and muscle strength was observed, as well as impaired neurotransmission and a significant decrease in the action potential. Furthermore, the structure of the gastrocnemius muscle was disturbed, and muscle fibers appeared broken based on microscopic observation with H&E staining. In the rats treated with AS-IV, the aforementioned observations were reversed. AS-IV could improve symptoms of muscle weakness and pathological changes in the gastrocnemius muscle and could improve the attenuation of the action potential of the gastrocnemius muscle and restore neurotransmission, thus indicating that AS-IV may exert a protective effect on EAMG rats.

The primary autoimmune antibody associated with MG onset is AChR-Ab, which targets the postsynaptic membrane of AChR, leading to disrupted ACh transmission and impaired NMJ function, resulting in symptoms of muscle weakness (58). The current treatment approach for MG primarily involves the use of acetylcholinesterase inhibitors, corticosteroids and immunosuppressants, which can alleviate symptoms in the majority of patients with MG (59). However, ~15% of patients with MG have been reported to show limited or no response to these therapies (60), while simultaneously enduring the burden of numerous adverse reactions (61,62). AS-IV, a natural medicinal compound derived from *A. membranaceus*, is a traditional Chinese medicine that presents advantages, such as cost-effectiveness and low toxicity (63,64). In the present study, the levels of AChR-Ab were increased in EAMG rats in response to modeling, but were reversed after AS-IV treatment, suggesting the potential for AS-IV to regulate AChR-Ab levels in EAMG rats. Nevertheless, ~20% of patients with MG do not exhibit AChR-Ab in their serum (65), and the severity of symptoms is not correlated with antibody levels (66-68), which presents challenges in diagnosis, treatment selection and evaluation of prognosis. The present findings indicated that AS-IV not only reduced serum AChR-Ab levels in EAMG rats, but also significantly improved the morphology and function of skeletal muscle mitochondria. It may be hypothesized that mitochondrial damage serves a role in MG, and AS-IV could exert its therapeutic effects by improving mitochondrial function.

The NMJ is a highly active site that requires a significant amount of energy to sustain the transmission of nerve impulses and muscle contraction (17). Mitochondria have a vital role in providing energy for these processes through the production of ATP (69). Furthermore, mitochondria serve a role in antioxidant defense and in the regulation of calcium ions (18). Certain proteins within mitochondria can also promote the aggregation of AChRs at the postsynaptic membrane (70). In summary, the proper functioning of mitochondria ensures the coordinated progression of NMJ activity and skeletal muscle physiology.

The pathological process of MG may be significantly influenced by mitochondrial dysfunction. Previous studies have shown mitochondrial accumulation and atypical abnormal ultrastructure in muscle biopsies obtained from patients with MG (15). Additionally, there is a deficiency of mitochondrial respiratory chain complexes in patients with MG (71). Mitochondrial dysfunction and depleted energy levels have also been observed in the muscle tissue of patients with MG (16). The impairment of mitochondria can diminish muscle energy production and trigger oxidative stress, further exacerbating symptoms of muscle weakness (72). Consequently, reversing mitochondrial damage, and restoring the normal structure and function of mitochondria, are crucial for effective MG treatment. In the present study, after modeling, compared with in the control group, the model group rats demonstrated a marked decrease in the number of mitochondria in the gastrocnemius muscle, along with incomplete mitochondrial structure, swelling and vacuolization, and there was a lack of cristae based on TEM. Subsequent administration of AS-IV at low or high doses led to an increase in mitochondrial quantity and pronounced improvement in mitochondrial structure, particularly in the high-dose group, where well-defined cristae and relatively intact mitochondrial structure were evident. These findings suggested that AS-IV may exert a protective effect against mitochondrial damage in EAMG.

The activity of ATPase can reflect the function of mitochondria. ATPase hydrolyzes ATP into ADP and phosphate, and releases energy for almost all essential cellular processes (73). In our previous study, myocyte damage alongside decreased Ca^{2+}/Mg^{2+}-ATP and Na^{+}/K^{+}-ATP enzyme activity were observed in the skeletal muscle of EAMG rats, indicative of abnormal energy metabolism in the skeletal muscle of EAMG rats, resulting in impaired muscle diastolic movement (19). COX, also known as mitochondrial respiratory chain complex IV, is one of the oxidases essential for mitochondrial respiratory function (74). Previous studies have shown that defects in the mitochondrial respiratory chain are important factors that interfere with cellular energy metabolism and are an important cause of skeletal muscle injury (75-77). In the present study, by staining frozen sections of the rat gastrocnemius muscle, the results showed that the model group had a reduced staining and markedly lower activity in the positively stained ATPase area, low COX activity, and a lower number of cells positive for both ATPase and COX activity, all of which were restored after treatment with AS-IV. These results further confirmed that AS-IV could reduce skeletal muscle injury in EAMG rats by improving mitochondrial energy metabolism.

Mitophagy is a process that selectively removes damaged or abnormal mitochondria and serves a crucial role in maintaining intracellular homeostasis (78). PINK1/Parkin is the classical pathway mediating mitophagy. PINK1 acts as a mitochondrial Ser/Thr kinase that recruits Parkin to depolarized mitochondria and interacts with the outer mitochondrial

membrane complex to regulate Parkin translocation and activation. Parkin acts as an E3 ubiquitin ligase and is typically located in the cytoplasm. In response to mitochondrial stress, it is rapidly recruited to damaged mitochondria, thereby phosphorylating the ubiquitin ligase p62 and promoting its binding to LC3 in the mitochondria to initiate mitophagy (79).

Apoptosis serves an important role in the regulation of homeostasis in the human body, and mitochondrial apoptosis is one of the major routes of apoptosis, involving a variety of key signaling molecules (80). Apoptosis-promoting Bax protein and apoptosis-inhibiting Bcl-2 protein, primarily localized on the mitochondria and endoplasmic reticulum, jointly regulate mitochondrial membrane permeability and apoptosis signal transmission. When cells are stimulated by apoptotic signals, Bax proteins excessively accumulate in the outer mitochondrial membrane, enhancing mitochondrial membrane permeability. This leads to the release of soluble proteins such as Cyt-C from the intermembrane space to the cytoplasm. Subsequently, Cyt-C can recruit and activate proenzymes of caspase 9, initiating the amplification of the caspase cascade effect, and further activating the cleavage of caspase 3 precursors, ultimately leading to the initiation of apoptosis (81,82).

A growing number of studies have confirmed the close association between mitophagy and the development of progressive myasthenic diseases, such as neurogenic distal myopathy and ALS (83,84). Similarly, mitochondrial apoptosis has a key role in several neurodegenerative and autoimmune diseases, such as AD, PD and rheumatoid arthritis (RA) (83-86). AS-IV has been reported to prevent dopaminergic neurodegeneration in PD by promoting mitophagy to inhibit astrocyte senescence (87). AS-IV also attenuates Schwann cell injury in diabetic peripheral neuropathy by promoting autophagy (88). In addition, AS-IV attenuates neuroinflammation and delays smooth muscle cell senescence in spinal cord injury by promoting autophagy (89,90). AS-IV has also been shown to exert its anti-apoptotic effects in several diseases via the regulation of key mitochondrial apoptotic signaling molecules, such as Bax/Bcl-2 and the caspase family of proteins (91-94). However, the involvement of mitophagy and apoptosis in the development of MG and the potential of AS-IV to mitigate skeletal muscle injury in MG through the regulation of mitophagy and apoptosis remains unclear.

In the present study, the results showed there was a decrease in the mRNA and protein expression levels of PINK1 and Parkin, as well as an increase in the expression of p62 in the skeletal muscle tissues of the EAMG rat model. The expression of LC3, as a marker of autophagy, holds significant importance. Additionally, the ratio of LC3II/LC3I is often used to measure the degree of autophagy (95). A significant reduction in LC3II/I was observed in the skeletal muscle of EAMG rats, along with a decrease in the number of autophagosomes observed by TEM in the model group, indicating a marked attenuation of mitophagy in the skeletal muscle of EAMG rats. Furthermore, the mRNA and protein expression levels of pro-apoptosis-related signaling molecules, such as Cyt-C, Bax, caspase 3 and caspase 9, were increased, whereas the expression levels of the apoptosis-suppressing protein Bcl-2 were decreased, leading to an elevated level of mitochondrial apoptosis. All of the aforementioned changes were reversed by AS-IV treatment. Therefore, these findings indicated that mitophagy was reduced and mitochondrial apoptosis was elevated in the skeletal muscle of EAMG rats, resulting in skeletal muscle cell damage. Conversely, AS-IV improved the morphology, structure and function of mitochondria by promoting mitophagy and inhibiting mitochondrial apoptosis. This effectively reduced the pathological damage to skeletal muscle and improved the symptoms in EAMG rats.

However, the present study has some limitations. In the present study, AS-IV could decrease the levels of AChR-Ab and alleviate aberrant mitophagy and apoptosis. However, the potential link between mitophagy, apoptosis and AChR-Ab remains unclear; investigating this association presents an intriguing question, and further exploration of this topic will be pursued in future research.

In conclusion, to the best of our knowledge, the present study was the first to demonstrate that AS-IV protected against EAMG in a rat model by modulating mitophagy and apoptosis. This resulted in an improvement in mitochondrial structure and function, as well as a reduction in gastrocnemius muscle damage. These findings provide novel insights into the potential mechanism of MG and highlight potential novel treatment strategies.

Acknowledgements

Not applicable.

Funding

The present study was supported by the Natural Science Foundation of Guangdong Province (grant no. 2023A1515011127), the Project in Key Fields of Universities in Guangdong Province (grant no 2021ZDZX2032) and the National Natural Science Foundation of China (grant no. 82374391).

Availability of data and materials

The data generated in the present study may be requested from the corresponding author.

Authors' contributions

JZ, JH, JL, QL and LK performed experiments. JZ, JH and JL wrote the manuscript. QL, LK, QJ, YL, HZha, HZho and PY contributed to analysis and interpretation of data. HZho and PY provided critical comments on the revision of the manuscript. YS and TC contributed to the conception, design and supervision of the study. YS provided funding. JZ, QL and LK confirm the authenticity of all the raw data. All authors have read and approved the final version of the manuscript.

Ethics approval and consent to participate

All experimental procedures were approved by the Animal Ethics Committee of Guangzhou University of Traditional Chinese Medicine (Guangzhou, China; approval no. A202005017).

Patient consent for publication

Not applicable.

Competing interests

The authors declare that they have no competing interests.

References

1. Payet CA, You A, Fayet OM, Dragin N, Berrih-Aknin S and Le Panse R: Myasthenia gravis: An acquired interferonopathy? Cells 11: 1218, 2022.
2. Gilhus NE, Tzartos S, Evoli A, Palace J, Burns TM and Verschuuren J: Myasthenia gravis. Nat Rev Dis Primers 5: 30, 2019.
3. Huijbers MG, Marx A, Plomp JJ, Le Panse R and Phillips WD: Advances in the understanding of disease mechanisms of autoimmune neuromuscular junction disorders. Lancet Neurol 21: 163-175, 2022.
4. Cortés-Vicente E, Álvarez-Velasco R, Segovia S, Paradas C, Casasnovas C, Guerrero-Sola A, Pardo J, Ramos-Fransi A, Sevilla T, López de Munain A, *et al*: Clinical and therapeutic features of myasthenia gravis in adults based on age at onset. Neurology 94: e1171-e1180, 2020.
5. Gilhus NE and Verschuuren JJ: Myasthenia gravis: Subgroup classification and therapeutic strategies. Lancet Neurol 14: 1023-1036, 2015.
6. Punga AR, Maddison P, Heckmann JM, Guptill JT and Evoli A: Epidemiology, diagnostics, and biomarkers of autoimmune neuromuscular junction disorders. Lancet Neurol 21: 176-188, 2022.
7. García Estévez DA and Pardo Fernández J: Myasthenia gravis. Update on diagnosis and therapy. Med Clin (Barc) 161: 119-127, 2023.
8. Mahic M, Bozorg A, DeCourcy J, Golden K, Gibson G, Taylor C and Scowcroft A: Physician- and patient-reported perspectives on myasthenia gravis in Europe: A real-world survey. Orphanet J Rare Dis 18: 169, 2023.
9. Petersson M, Feresiadou A, Jons D, Ilinca A, Lundin F, Johansson R, Budzianowska A, Roos AK, Kågström V, Gunnarsson M, *et al*: Patient-Reported symptom severity in a nationwide myasthenia gravis cohort: Cross-sectional analysis of the swedish GEMG study. Neurology 97: e1382-1391, 2021.
10. Verschuuren JJ, Palace J, Murai H, Tannemaat MR, Kaminski HJ and Bril V: Advances and ongoing research in the treatment of autoimmune neuromuscular junction disorders. Lancet Neurol 21: 189-202, 2022.
11. Walker BR and Moraes CT: Nuclear-mitochondrial interactions. Biomolecules 12: 427, 2022.
12. de Beauchamp L, Himonas E and Helgason GV: Mitochondrial metabolism as a potential therapeutic target in myeloid leukaemia. Leukemia 36: 1-12, 2022.
13. Xiang L, Shao Y and Chen Y: Mitochondrial dysfunction and mitochondrion-targeted therapeutics in liver diseases. J Drug Target 29: 1080-1093, 2021.
14. Yang X, Xue P, Yuan M, Xu X, Wang C, Li W, Machens HG and Chen Z: SESN2 protects against denervated muscle atrophy through unfolded protein response and mitophagy. Cell Death Dis 12: 805, 2021.
15. Martignago S, Fanin M, Albertini E, Pegoraro E and Angelini C: Muscle histopathology in myasthenia gravis with antibodies against MuSK and AChR. Neuropathol Appl Neurobiol 35: 103-110, 2009.
16. Shichijo K, Mitsui T, Kunishige M, Kuroda Y, Masuda K and Matsumoto T: Involvement of mitochondria in myasthenia gravis complicated with dermatomyositis and rheumatoid arthritis: A case report. Acta Neuropathol 109: 539-542, 2005.
17. Sousa-Soares C, Noronha-Matos JB and Correia-de-Sá P: Purinergic tuning of the tripartite neuromuscular synapse. Mol Neurobiol 60: 4084-4104, 2023.
18. Ferrari R, Rodrigues-Simioni L and da Cruz Höfling MA: Guanidine affects differentially the twitch response of diaphragm, extensor digitorum longus and soleus nerve-muscle preparations of mice. Molecules 17: 7503-7522, 2012.
19. Jiao W, Hu F, Li J, Song J, Liang J, Li L, Song Y, Chen Z, Li Q and Ke L: Qiangji Jianli Decoction promotes mitochondrial biogenesis in skeletal muscle of myasthenia gravis rats via AMPK/PGC-1α signaling pathway. Biomed Pharmacother 129: 110482, 2020.
20. Ke L, Li Q, Song J, Jiao W, Ji A, Chen T, Pan H and Song Y: The mitochondrial biogenesis signaling pathway is a potential therapeutic target for myasthenia gravis via energy metabolism (Review). Exp Ther Med 22: 702, 2021.
21. Li L, Cai D, Zhong H, Liu F, Jiang Q, Liang J, Li P, Song Y, Ji A, Jiao W, *et al*: Mitochondrial dynamics and biogenesis indicators may serve as potential biomarkers for diagnosis of myasthenia gravis. Exp Ther Med 23: 307, 2022.
22. Song J, Lei X, Jiao W, Song Y, Chen W, Li J and Chen Z: Effect of Qiangji Jianli decoction on mitochondrial respiratory chain activity and expression of mitochondrial fusion and fission proteins in myasthenia gravis rats. Sci Rep 8: 8623, 2018.
23. Zheng Z, Guo C, Li M, Yang L, Liu P, Zhang X, Liu Y, Guo X, Cao S, Dong Y, *et al*: Hypothalamus-habenula potentiation encodes chronic stress experience and drives depression onset. Neuron 110: 1400-1415.e6, 2022.
24. Su L, Zhang J, Gomez H, Kellum JA and Peng Z: Mitochondria ROS and mitophagy in acute kidney injury. Autophagy 19: 401-414, 2023.
25. Gupta R, Ambasta RK and Pravir K: Autophagy and apoptosis cascade: Which is more prominent in neuronal death? Cell Mol Life Sci 78: 8001-8047, 2021.
26. Lai Y, Xu X, Zhu Z and Hua Z: Highly efficient siRNA transfection in macrophages using apoptotic body-mimic Ca-PS lipopolyplex. Int J Nanomedicine 13: 6603-6623, 2018.
27. Zhang J, Ma G, Guo Z, Yu Q, Han L, Han M and Zhu Y: Study on the apoptosis mediated by apoptosis-inducing-factor and influencing factors of bovine muscle during postmortem aging. Food Chem 266: 359-367, 2018.
28. Piras A, Schiaffino L, Boido M, Valsecchi V, Guglielmotto M, De Amicis E, Puyal J, Garcera A, Tamagno E, Soler RM and Vercelli A: Inhibition of autophagy delays motoneuron degeneration and extends lifespan in a mouse model of spinal muscular atrophy. Cell Death Dis 8: 3223, 2017.
29. Kuno A, Hosoda R, Sebori R, Hayashi T, Sakuragi H, Tanabe M and Horio Y: Resveratrol ameliorates mitophagy disturbance and improves cardiac pathophysiology of Dystrophin-deficient mdx Mice. Sci Rep 8: 15555, 2018.
30. De Palma C, Morisi F, Cheli S, Pambianco S, Cappello V, Vezzoli M, Rovere-Querini P, Moggio M, Ripolone M, Francolini M, *et al*: Autophagy as a new therapeutic target in Duchenne muscular dystrophy. Cell Death Dis 3: e418, 2012.
31. Bloemberg D and Quadrilatero J: Autophagy, apoptosis, and mitochondria: Molecular integration and physiological relevance in skeletal muscle. Am J Physiol Cell Physiol 317: C111-C130, 2019.
32. Jing H, Xie R, Bai Y, Duan Y, Sun C, Wang Y, Cao R, Ling Z and Qu X: The mechanism actions of astragaloside IV prevents the progression of hypertensive heart disease based on network pharmacology and experimental pharmacology. Front Pharmacol 12: 755653, 2021.
33. Song J, Li Q, Ke L, Liang J, Jiao W, Pan H, Li Y, Du Q, Song Y, Ji A, *et al*: Qiangji jianli decoction alleviates hydrogen peroxide-induced mitochondrial dysfunction via regulating mitochondrial dynamics and biogenesis in L6 myoblasts. Oxid Med Cell Longev 2021: 6660616, 2021.
34. Costa IM, Lima FOV, Fernandes LCB, Norrara B, Neta FI, Alves RD, Cavalcanti JRLP, Lucena EES, Cavalcante JS, Rego ACM, *et al*: Astragaloside IV supplementation promotes A neuroprotective effect in experimental models of neurological disorders: A systematic review. Curr Neuropharmacol 17: 648-665, 2019.
35. Zhu T, Wang L, Wang LP and Wan Q: Therapeutic targets of neuroprotection and neurorestoration in ischemic stroke: Applications for natural compounds from medicinal herbs. Biomed Pharmacother 148: 112719, 2022.
36. Zhong Y, Liu W, Xiong Y, Li Y, Wan Q, Zhou W, Zhao H, Xiao Q and Liu D: Astragaloside IV alleviates ulcerative colitis by regulating the balance of Th17/Treg cells. Phytomedicine 104: 154287, 2022.
37. Bolduc JA, Collins JA and Loeser RF: Reactive oxygen species, aging and articular cartilage homeostasis. Free Radic Biol Med 132: 73-82, 2019.
38. Jiang B, Yang YJ, Dang WZ, Li H, Feng GZ, Yu XC, Shen XY and Hu XG: Astragaloside IV reverses simvastatin-induced skeletal muscle injury by activating the AMPK-PGC-1α signalling pathway. Phytother Res 34: 1175-1184, 2020.
39. National Research Council (US) Committee for the Update of the Guide for the Care and Use of Laboratory Animals: Guide for the care and use of laboratory animals. 8th edition. Washington (DC), National Academies Press (US), 2011.

40. Baggi F, Annoni A, Ubiali F, Longhi R, Milani M, Mantegazza R, Cornelio F and Antozzi C: Immunization with rat-, but not Torpedo-derived 97-116 peptide of the AChR alpha-subunit induces experimental myasthenia gravis in Lewis rat. Ann N Y Acad Sci 998: 391-394, 2003.
41. He X, Zhou S, Ji Y, Zhang Y, Lv J, Quan S, Zhang J, Zhao X, Cui W, Li W, *et al*: Sorting nexin 17 increases low-density lipoprotein receptor-related protein 4 membrane expression: A novel mechanism of acetylcholine receptor aggregation in myasthenia gravis. Front Immunol 13: 916098, 2022.
42. Wang CC, Li H, Zhang M, Li XL, Yue LT, Zhang P, Zhao Y, Wang S, Duan RN, Li YB and Duan RS: Caspase-1 inhibitor ameliorates experimental autoimmune myasthenia gravis by innate dendric cell IL-1-IL-17 pathway. J Neuroinflammation 12: 118, 2015.
43. Claussen GC, Fesenmeier JT, Hah JS, Brooks J and Oh SJ: The accessory nerve repetitive nerve stimulation test: A valuable second-line test in myasthenia gravis. Eur J Neurol 2: 492-497, 1995.
44. Nie Q, Zhu L, Zhang L, Leng B and Wang H: Astragaloside IV protects against hyperglycemia-induced vascular endothelial dysfunction by inhibiting oxidative stress and Calpain-1 activation. Life Sci 232: 116662, 2019.
45. Liu YL, Zhang QZ, Wang YR, Fu LN, Han JS, Zhang J and Wang BM: Astragaloside IV improves High-Fat Diet-Induced hepatic steatosis in nonalcoholic fatty liver disease rats by regulating inflammatory factors level via TLR4/NF-κB signaling pathway. Front Pharmacol 11: 605064, 2020.
46. Yang J, Wang HX, Zhang YJ, Yang YH, Lu ML, Zhang J, Li ST, Zhang SP and Li G: Astragaloside IV attenuates inflammatory cytokines by inhibiting TLR4/NF-κB signaling pathway in isoproterenol-induced myocardial hypertrophy. J Ethnopharmacol 150: 1062-1070, 2013.
47. Laferriere CA and Pang DS: Review of intraperitoneal injection of sodium pentobarbital as a method of euthanasia in laboratory rodents. J Am Assoc Lab Anim Sci 59: 254-263, 2020.
48. Livak KJ and Schmittgen TD: Analysis of relative gene expression data using real-time quantitative PCR and the 2(-Delta Delta C(T)) method. Methods 25: 402-408, 2001.
49. van der Bliek AM, Sedensky MM and Morgan PG: Cell biology of the mitochondrion. Genetics 207: 843-871, 2017.
50. Mansilla N, Racca S, Gras DE, Gonzalez DH and Welchen E: The complexity of mitochondrial Complex IV: An update of cytochrome c oxidase biogenesis in plants. Int J Mol Sci 19: 662, 2018.
51. Ni GX, Liang C, Wang J, Duan CQ, Wang P and Wang YL: Astragaloside IV improves neurobehavior and promotes hippocampal neurogenesis in MCAO rats though BDNF-TrkB signaling pathway. Biomed Pharmacother 130: 110353, 2020.
52. Shi YH, Zhang XL, Ying PJ, Wu ZQ, Lin LL, Chen W, Zheng GQ and Zhu WZ: Neuroprotective effect of Astragaloside IV on cerebral Ischemia/Reperfusion injury rats through Sirt1/Mapt pathway. Front Pharmacol 12: 639898, 2021.
53. Yin Y, Qu H, Yang Q, Fang Z and Gao R: Astragaloside IV alleviates Schwann cell injury in diabetic peripheral neuropathy by regulating microRNA-155-mediated autophagy. Phytomedicine 92: 153749, 2021.
54. Kuo YC, Chen IY and Rajesh R: Astragaloside IV- and nesfatin-1-encapsulated phosphatidylserine liposomes conjugated with wheat germ agglutinin and leptin to activate anti-apoptotic pathway and block phosphorylated tau protein expression for Parkinson's disease treatment. Mater Sci Eng C Mater Biol Appl 129: 112361, 2021.
55. Tian Y, Jin S, Promes V, Liu X and Zhang Y: Astragaloside IV and echinacoside benefit neuronal properties via direct effects and through upregulation of SOD1 astrocyte function in vitro. Naunyn Schmiedebergs Arch Pharmacol 394: 1019-1029, 2021.
56. Smith EF, Shaw PJ and De Vos KJ: The role of mitochondria in amyotrophic lateral sclerosis. Neurosci Lett 710: 132933, 2019.
57. Attia M, Maurer M, Robinet M, Le Grand F, Fadel E, Le Panse R, Butler-Browne G and Berrih-Aknin S: Muscle satellite cells are functionally impaired in myasthenia gravis: Consequences on muscle regeneration. Acta Neuropathol 134: 869-888, 2017.
58. Truffault F, de Montpreville V, Eymard B, Sharshar T, Le Panse R and Berrih-Aknin S: Thymic germinal centers and corticosteroids in myasthenia gravis: An immunopathological study in 1035 cases and a critical review. Clin Rev Allergy Immunol 52: 108-124, 2017.
59. Menon D and Bril V: Pharmacotherapy of generalized myasthenia gravis with special emphasis on newer biologicals. Drugs 82: 865-887, 2022.
60. Mantegazza R and Antozzi C: When myasthenia gravis is deemed refractory: Clinical signposts and treatment strategies. Ther Adv Neurol Disord 11: 1756285617749134, 2018.
61. Lorenzoni PJ, Kay CSK, Zanlorenzi MF, Ducci RD, Werneck LC and Scola RH: Myasthenia gravis and azathioprine treatment: Adverse events related to thiopurine S-methyl-transferase (TPMT) polymorphisms. J Neurol Sci 412: 116734, 2020.
62. Tao X, Wang W, Jing F, Wang Z, Chen Y, Wei D and Huang X: Long-term efficacy and side effects of low-dose tacrolimus for the treatment of Myasthenia Gravis. Neurol Sci 38: 325-330, 2017.
63. Stępnik K, Kukula-Koch W, Plazinski W, Gawel K, Gaweł-Bęben K, Khurelbat D and Boguszewska-Czubara A: Significance of astragaloside IV from the roots of astragalus mongholicus as an acetylcholinesterase inhibitor-from the computational and biomimetic analyses to the in vitro and in vivo studies of safety. Int J Mol Sci 24: 9152, 2023.
64. Yuan F, Yang Y, Liu L, Zhou P, Zhu Y, Chai Y, Chen K, Tang W, Huang Q and Zhang C: Research progress on the mechanism of astragaloside IV in the treatment of asthma. Heliyon 9: e22149, 2023.
65. Rivner MH, Pasnoor M, Dimachkie MM, Barohn RJ and Mei L: Muscle-Specific tyrosine kinase and myasthenia gravis owing to other antibodies. Neurol Clin 36: 293-310, 2018.
66. Howard FM Jr, Lennon VA, Finley J, Matsumoto J and Elveback LR: Clinical correlations of antibodies that bind, block, or modulate human acetylcholine receptors in myasthenia gravis. Ann N Y Acad Sci 505: 526-538, 1987.
67. Lindstrom JM, Seybold ME, Lennon VA, Whittingham S and Duane DD: Antibody to acetylcholine receptor in myasthenia gravis. Prevalence, clinical correlates, and diagnostic value. Neurology 26: 1054-1059, 1976.
68. Gilhus NE, Skeie GO, Romi F, Lazaridis K, Zisimopoulou P and Tzartos S: Myasthenia gravis-autoantibody characteristics and their implications for therapy. Nature Rev Neurology 12: 259-268, 2016.
69. Anagnostou ME and Hepple RT: Mitochondrial mechanisms of neuromuscular junction degeneration with aging. Cells 9: 197, 2020.
70. Xiao Y, Zhang J, Shu X, Bai L, Xu W, Wang A, Chen A, Tu WY, Wang J, Zhang K, *et al*: Loss of mitochondrial protein CHCHD10 in skeletal muscle causes neuromuscular junction impairment. Hum Mol Genet 29: 1784-1796, 2020.
71. Finsterer J, Oberman I and Reitner A: Respiratory chain complex-I defect mimicking myasthenia. Metab Brain Dis 17: 41-46, 2002.
72. Jang YC, Lustgarten MS, Liu Y, Muller FL, Bhattacharya A, Liang H, Salmon AB, Brooks SV, Larkin L, Hayworth CR, *et al*: Increased superoxide in vivo accelerates age-associated muscle atrophy through mitochondrial dysfunction and neuromuscular junction degeneration. FASEB 24: 1376-1390, 2010.
73. Holper L, Ben-Shachar D and Mann JJ: Multivariate meta-analyses of mitochondrial complex I and IV in major depressive disorder, bipolar disorder, schizophrenia, Alzheimer disease, and Parkinson disease. Neuropsychopharmacology 44: 837-849, 2019.
74. Ferreira N, Andoniou CE, Perks KL, Ermer JA, Rudler DL, Rossetti G, Periyakaruppiah A, Wong JKY, Rackham O, Noakes PG, *et al*: Murine cytomegalovirus infection exacerbates complex IV deficiency in a model of mitochondrial disease. PLoS Genet 16: e1008604, 2020.
75. Hatakeyama H and Goto YI: Respiratory chain complex disorganization impairs mitochondrial and cellular integrity: Phenotypic variation in cytochrome c oxidase deficiency. Am J Pathol 187: 110-121, 2017.
76. Wang XL, Feng ST, Wang ZZ, Chen NH and Zhang Y: Role of mitophagy in mitochondrial quality control: Mechanisms and potential implications for neurodegenerative diseases. Pharmacol Res 165: 105433, 2021.
77. Chu CT: Mechanisms of selective autophagy and mitophagy: Implications for neurodegenerative diseases. Neurobiol Dis 122: 23-34, 2019.
78. Evans CS and Holzbaur ELF: Autophagy and mitophagy in ALS. Neurobiol Dis 122: 35-40, 2019.
79. Carrascoso I, Sánchez-Jiménez C, Silion E, Alcalde J and Izquierdo JM: A heterologous cell model for studying the role of T-Cell intracellular antigen 1 in welander distal myopathy. Mol Cell Biol 39: e00299-18, 2019.
80. Wang TS, Coppens I, Saorin A, Brady NR and Hamacher-Brady A: Endolysosomal targeting of mitochondria is integral to BAX-Mediated mitochondrial permeabilization during apoptosis signaling. Developmental cell 53: 627-645.e7, 2020.

81. Yin W, Li R, Feng X and James Kang Y: The Involvement of cytochrome c Oxidase in mitochondrial fusion in primary cultures of neonatal rat cardiomyocytes. Cardiovasc Toxicol 18: 365-373, 2018.
82. Wang XR, Wang C, Wang XW, Qian LX, Chi Y, Liu SS, Liu YQ and Wang XW: The functions of caspase in whitefly Bemisia tabaci apoptosis in response to ultraviolet irradiation. Insect Mol Biol 27: 739-751, 2018.
83. Huang G, Li H and Zhang H: Abnormal expression of mitochondrial ribosomal proteins and their encoding genes with cell apoptosis and diseases. Int J Mol Sci 21: 8879, 2020.
84. Hazafa A, Batool A, Ahmad S, Amjad M, Chaudhry SN, Asad J, Ghuman HF, Khan HM, Naeem M and Ghani U: Humanin: A mitochondrial-derived peptide in the treatment of apoptosis-related diseases. Life Sci 264: 118679, 2021.
85. Bock FJ and Tait SWG: Mitochondria as multifaceted regulators of cell death. Nat Rev Mol Cell Biol 21: 85-100, 2020.
86. Zheng M, Kuang N, Zeng X, Wang J, Zou Y and Fu Y: Daphnetin induces apoptosis in fibroblast-like synoviocytes from collagen-induced arthritic rats mainly via the mitochondrial pathway. Cytokine 133: 155146, 2020.
87. Xia ML, Xie XH, Ding JH, Du RH and Hu G: Astragaloside IV inhibits astrocyte senescence: Implication in Parkinson's disease. J Neuroinflammation 17: 105, 2020.
88. Yin Y, Qu H, Yang Q, Fang Z and Gao R: Corrigendum to 'Astragaloside IV alleviates Schwann cell injury in diabetic peripheral neuropathy by regulating microRNA-155-mediated autophagy'. Phytomedicine 97: 153916, 2022.
89. Lin J, Pan X, Huang C, Gu M, Chen X, Zheng X, Shao Z, Hu S, Wang B, Lin H, *et al*: Dual regulation of microglia and neurons by Astragaloside IV-mediated mTORC1 suppression promotes functional recovery after acute spinal cord injury. J Cell Mol Med 24: 671-685, 2020.
90. Li H, Xu J, Zhang Y, Hong L, He Z, Zeng Z and Zhang L: Astragaloside IV alleviates senescence of vascular smooth muscle cells through activating Parkin-mediated mitophagy. Hum Cell 35: 1684-1696, 2022.
91. Feng M, Lv J, Zhang C, Chen D, Guo H, Tu Y, Su L and Wang Z: Astragaloside IV protects sepsis-induced acute kidney injury by attenuating mitochondrial dysfunction and apoptosis in renal tubular epithelial cells. Curr Pharm Des 28: 2825-2834, 2022.
92. Li H, Yao C, Shi K, Zhao Y, Du J, Hu D and Liu Z: Astragaloside IV attenuates hypoxia/reoxygenation injury-induced apoptosis of type II alveolar epithelial cells through miR-21-5p. Bioengineered 12: 7747-7754, 2021.
93. Wang F, Zhao Y, Chen S, Chen L, Sun L, Cao M, Li C and Zhou X: Astragaloside IV alleviates ammonia-induced apoptosis and oxidative stress in bovine mammary epithelial cells. Int J Mol Sci 20: 600, 2019.
94. Qin S, Yin J, Huang S, Lin J, Fang Z, Zhou Y and Huang K: Astragaloside IV protects ethanol-induced gastric mucosal injury by preventing mitochondrial oxidative stress and the activation of mitochondrial pathway apoptosis in rats. Front Pharmacol 10: 894, 2019.
95. Yoshii SR and Mizushima N: Monitoring and measuring autophagy. Int J Mol Sci 18: 1865, 2017.